Directed Coevolution of Stability and Catalytic Activity in Calcium-free Subtilisin†

Susan L. Strausberg, Biao Ruan, Kathryn E. Fisher, Patrick A. Alexander, and Philip N. Bryan*

Center for Advanced Research in Biotechnology, University of Maryland Biotechnology Institute, 9600 Gudelsky Drive, Rockville, Maryland 20850

Received October 13, 2004; Revised Manuscript Received December 17, 2004

ABSTRACT: We have coevolved high activity and hyperstability in subtilisin by sequentially randomizing 12 amino acid positions in calcium-free subtilisin. The optimal amino acid for each randomized site was chosen based on stability and catalytic properties and became the parent clone for the next round of mutagenesis. Together, the 12 selected mutations increased the half-life of calcium-free subtilisin at elevated temperature by 15 000-fold. The catalytic properties of the mutants were examined against a range of substrates. In general, only mutations occurring at or near the substrate-binding surface have measurable effects on catalytic constants. No direct influence of stability on catalytic properties was observed. A high-stability mutant, Sbt140, was a more efficient enzyme in terms of k_{cat}/K_m than a commercial version of subtilisin across a range of substrates but had a lower k_{cat} against tight-binding substrates. The reason for this behavior was discerned by examining microscopic rate constants for the hydrolysis of a tight-binding peptide substrate. Burst kinetics were observed for this substrate, indicating that acylation is not rate-limiting. Although acylation occurs at the rate of substrate binding, k_{cat} is attenuated by the slow release of the N-terminal product. Natural evolution appears to have optimized catalytic activity against a range of sequences by achieving a balance between substrate binding and the rate of release of the N-terminal product.

Subtilisin BPN′ from *Bacillus amyloliquefaciens* is a secreted, serine protease, which degrades proteins in the extracellular environment and provides amino acids to the *Bacillus* (*1*−*3*). It is an important industrial enzyme as well as a model system for protein engineering studies (*4*). Subtilisins from mesophilic organisms are generally highly efficient catalysts, turning over a broad spectrum of protein substrates at rates exceeding 10^6 M^{-1} s^{-1} at 25 °C (*5*). Thermophilic subtilisins generally are less efficient. One of the practical goals of protein-engineering efforts is to create subtilisins that are both highly stable and highly efficient catalysts (*6*, *7*). Here, we evolve a hyperstable subtilisin and measure catalytic properties as a function of stabilizing mutation.

The variants examined here lack the calcium-binding loop A of natural subtilisins. Site A is formed from a nine amino acid bubble in the last turn of an α helix, comprising amino acids 63−85 (helix C) (*8*). In previous work, we have shown that deleting amino acids 75−83 creates an uninterrupted helix with normal helical geometry over its entire length and abolishes the calcium-binding potential at site A (*9*−*11*). Nevertheless, regions of subtilisin that were adjacent to the 75−83 loop have lost many favorable interactions. Consequently, a number of compensating mutations were identified and introduced into the deletion mutant to restore stability (Q2K,[1] S3C, P5S, K43N, M50F, A73L, Q206C, Y217K, N218S, and Q271E). This mutant is referred to as Sbt88. The directed evolution of calcium-free subtilisin has been described previously (*12*). The X-ray crystal structure of Sbt88 subtilisin (PDB ID 1DUI) is described in Almog et al. (*13*).

The loop-deleted background has become a platform for further engineering because stability can be studied independent of calcium binding and because of the potential usefulness of chelant-stable subtilisins for biotechnological applications. This paper describes the identification of 12 additional stabilizing mutations by site-directed random mutagenesis in the loop-deleted background. Collectively, the 12 mutations increase enzymatic half-life by 15 000 times at temperatures ≥65 °C. The goal of this paper is to examine interrelationships between stability and catalytic properties.

MATERIALS AND METHODS

Expression and Purification of Subtilisins. The subtilisin gene from *Bacillus amyloliquefaciens* (subtilisin BPN′) has been cloned, sequenced, and expressed at high levels from its natural promoter sequences in *Bacillus subtilis* (*2*, *3*). All mutant genes (encoding the signal peptide, prodomain, and mature subtilisin) were recloned into a pUB110-based expression plasmid and used to transform *B. subtilis*. The *B. subtilis* strain used as the host contains a chromosomal deletion of its subtilisin gene and therefore produces no background wild-type activity (*14*). Subtilisin varaints were expressed in a 5 L New Brunswick fermentor at a level of ≥200 mg/L. Fermentation conditions and purification were as described (*15*). The enzyme concentration (*E*) was determined using E 0.1% = 1.17 at 280 nm (*1*). For variants

† This work was supported by NIH Grant GM42560.

* To whom correspondence should be addressed. E-mail: bryan@umbi.umd.edu. Telephone: 301-738-6220. Fax: 301-738-6255.

[1] A shorthand for denoting amino acid substitutions employs the single-letter amino acid code as follows: Q2K denotes the change of glutamine at position 2 to lysine.

10.1021/bi047806m CCC: $30.25
Published on Web 02/15/2005

that contain a Y217 mutation, the *E* 0.1% at 280 nm was calculated to be 1.12 based on the loss of one Tyr residue (*16*).

Construction of Active Calcium-free Subtilisin Genes. Because calcium-free subtilisin is lethal to *Escherichia coli*, mutagenesis to create genes for active calcium-free subtilisin had to be carried out in such a way to prevent leaky expression in the steps in which *E. coli* was used as a host. To separate the Δ75−83 subtilisin gene into nonfunctional pieces, an *Mlu* I site was introduced at the junction between the prosequence and the mature portion in the expression plasmid for the inactive calcium-free subtilisin Sbt15 (pS15) (*9*). Subtilisin Sbt15 is inactive because of a mutation of S221C. An *Mlu* I site was also introduced into M13 mp19. The portion of Sbt15 subtilisin gene encoding only mature subtilisin was then subcloned as a 1.2-kb *Mlu* I to *Sal* I fragment into the altered M13 mp19. The m13 clone was mutagenized to convert cysteine 221 back to serine. This construction was incapable of producing active subtilisin because it contained neither the expression signals nor the prosequence. The mutagenized *Mlu* I to *Sal* I fragment, containing the mature portion of the active gene, was ligated into the expression plasmid and cloned directly into *B. subtilis*.

Directed Mutagenesis and Screening for Increased Stability. Site-directed mutagenesis was performed on subtilisin genes with oligonucleotides, which were degenerate at a chosen codon using QuikChange (Stratagene) mutagenesis kits according to the instructions of the manufacturer. The degenerate codon contained all combinations of the sequence NNB, where N is any of the four nucleotides and B is T, C, or G. The 48 codons represented in this population encode for all 20 amino acids but exclude the ochre and amber termination codons. The mutagenized gene was ligated into an expression plasmid and used to transform *B. subtilis*. To have a 98% chance of finding an amino acid represented only once in the population of codons NNB (W, E, Q, or M), one must screen about 200 mutant clones. Codons for all other amino acids are represented by at least two codons in the population and would require screening of about 100 mutant clones to have a 98% chance of being represented in the mutant population. A total of 200−300 clones were screened in each experiment.

Mutant clones were grown in microtiter dishes and screened for proteolytic activity using 1% skim milk. A total of 50 μL of 2% yeast extract was dispensed in each of the 96 wells of a microtiter dish. Each well was inoculated with a *Bacillus* transformant and incubated at 37 °C with shaking. After 18 h of growth, 5 μL of culture was diluted into 95 μL of 100 mM tris(hydroxymethyl)aminomethane (Tris)[2]-HCl and 100 mM NaCl at pH 8.0 and 1% skim milk in a second microtiter dish. The wells in which the turbidity (absorbency at 600 nM) decreased the fastest were presumed to contain the most active subtilisin mutants.

Determination of Inactivation Rates. The kinetics of inactivation were determined as follows. Subtilisin at a 1 μM concentration was dispensed in aliquots of 0.5 mL into 1 mL glass test tubes and covered with Parafilm. The tubes were placed in a circulating water bath at the appropriate temperature. At each time point, a tube was removed and quickly transferred to an ice bath. A 10 μL aliquot was removed, and residual activity was assayed in 990 μL of 1 mM succinyl-L-Ala-L-Ala-L-Pro-L-Phe-*p*-nitroanilide (sAAPF-pNA), 0.1 M Tris-HCl at pH 8.0, and 0.1 M NaCl. The inactivation time course was followed over four half-lives (*17*).

Kinetic Measurements. Steady-state assays of the hydrolysis of sAAPF-pNA were as described by DelMar et al. (*18*). Succinyl-DVRAF-7-amino-4-methylcoumarin (AMC) was purchased from AnaSpec Inc. The concentrations of the AMC substrates were determined by absorbency at 324 nm using an extinction coefficient of 16 mM^{-1} cm^{-1}. Reaction kinetics of AMC substrates were measured using a KinTek stopped-flow model SF2001 (excitation $\lambda = 380$ nm, and emission = 400 nm cutoff filter). A stock solution of enzyme at a concentration of 2 mM in 10 mM KP_i at pH 5.7, 100 mM NaCl, and 50% glycerol was prepared for kinetic studies. Immediately prior to stop-flow mixing, the enzyme was diluted into 100 mM Tris-HCl at pH 8.3 and 100 mM NaCl and placed in syringe A of the SF2000. A solution of the substrate in the same buffer was place in syringe B. Solutions were equilibrated at 25 °C. Fluorescence data were collected after one to one mixing of the two solutions. For measurements of single turnover kinetics, the final enzyme concentration was varied from ∼0.5−20 μM with a constant substrate concentration of 50 pM. Typically, 10−15 kinetics traces were collected for each [*E*]. Kinetic mechanisms were simulated using KinTekSim (*19*, *20*), which was obtained from the KinTek Corporation website (www.kintek-corp.com).

RESULTS

Directed Mutagenesis and Screening. A total of 12 amino acid positions in Sbt88 subtilisin (Table 1) were chosen for random mutagenesis based on earlier studies. Amino acid position and references are as follows: S9 (*7*); I31 (*21*), E156 (*22*, *23*), G166 (*24*, *25*), G169 (*16*, *26*), S188 (*25*), N212 (*27*), A216 (*28*), Y217, (*16*, *26*), N218 (*29*), M222 (*30*), and T254 (*25*) (Table 1 and Figure 1). These were the only sites screened, although positions 8, 14, 27, 53, 63, 89, 109, 116, 118, 131, 161, 170, 172, 181, 194, 195, 213, and 256 would also have been good candidates based on earlier reports (*7*, *25*, *31*−*34*).

Generating and screening subtilisin variants involved *in vitro* random mutagenesis at each site of the Sbt88 subtilisin gene, expression of mutated genes in *B. subtilis*, and screening for activity versus casein as described in the Materials and Methods. Once preliminary identification of an active mutant was made from the microtiter dish assay, the corresponding *Bacillus* clone was grown for further analysis. The DNA sequence of the mutagenized site was determined for each clone confirmed to produce a high level of casein activity. Active mutants were further analyzed for stability and sAAPF-pNA activity.

The kinetics of thermal inactivation were measured in 100 mM Tris-HCl at pH 8.3 and 100 mM NaCl at temperatures from 65 to 75 °C. The rate of inactivation at

[2] Abbreviations: sAAF-AMC, succinyl-Ala-L-Ala-L-Phe-7-amino-4-methylcoumarin; sAAPF-pNA, succinyl-L-Ala-L-Ala-L-Pro-L-Phe-*p*-nitroanilide; sDVRAF-AMC, succinyl-L-Asp-L-Val-L-Arg-L-Ala-L-Phe-7-amino-4-methylcoumarin; $t_{1/2}$, half-life for a kinetic experiment; Tris, tris(hydroxymethyl)aminomethane.

Table 1: Mutation in Subtilisin[a]

mutation	Sbt88	Sbt98	Sbt99	Sbt103	Sbt107	Sbt109	Sbt110	Sbt116	Sbt140	Sbt151	Sbt153	Sbt184
Q2K	×	×	×	×	×	×	×	×	×	×	×	×
S3C	×	×	×	×	×	×	×	×	×	×	×	×
P5S	×	×	×	×	×	×	×	×	×	×	×	×
S9A										×	×	×
I31L						×	×	×	×	×	×	×
K43N	×	×	×	×	×	×	×	×	×	×	×	×
M50F	×	×	×	×	×	×	×	×	×	×	×	×
A73L	×	×	×	×	×	×	×	×	×	×	×	×
Δ75−83	×	×	×	×	×	×	×	×	×	×	×	×
E156S			×	×	×	×	×	×	×	×	×	×
G166S							×	×	×	×	×	×
A169A		×	×	×	×	×	×	×	×	×	×	×
S188P									×	×	×	×
Q206C	×	×	×	×	×	×	×	×	×	×	×	×
N212G								×	×	×	×	×
Y217L				×	×	×	×	×	×	×	×	×
A216E											×	×
N218S	×	×	×	×	×	×	×	×	×	×	×	×
M222Q												×
T254A					×	×	×	×	×	×	×	×
Q271E	×	×	×	×	×	×	×	×	×	×	×	×

[a] The × denotes that a variant subtilisin contains a specified mutation.

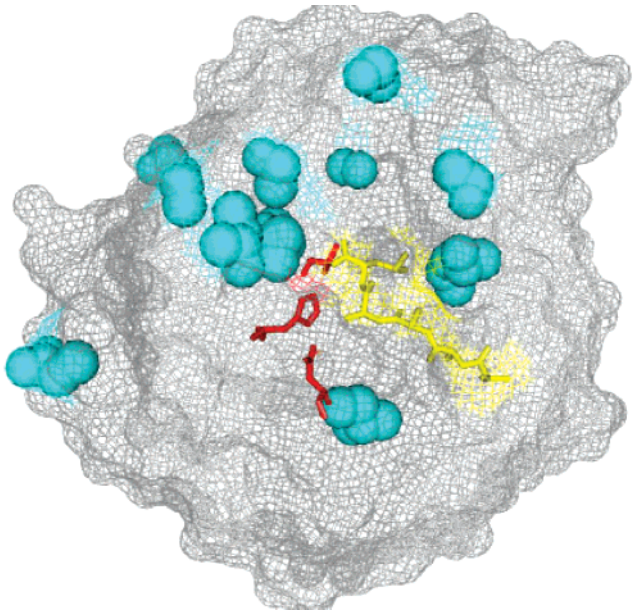

FIGURE 1: Structure of subtilisin S221A mutant of subtilisin Sbt110 (Gary Gilliland, manuscript in preparation). Sites of random mutation are shown by the cyan spheres. Active-site residues D32, H64, and S221 are shown in red. Pentapeptide AAAAL bound to the binding cleft is shown in yellow.

elevated temperatures and low concentrations (e.g., ≤ 1 μM) is characterized by a single-exponential decay curve, whose time constant is determined predominantly by the rate of subtilisin unfolding. Thus, mutations that decrease the rate of inactivation under these conditions can be considered to have increased the activation energy of unfolding (*15*, *17*).

Steady-state kinetic parameters against the peptide substrate sAAPF-pNA were determined in 100 mM Tris-HCl at pH 8.3 and 100 mM NaCl at 25 °C. The optimal amino acid for each randomized site was chosen based on stability and catalytic properties and became the parent clone for the next round of mutagenesis. The order of mutation was chosen arbitrarily and is shown in Table 2. No wild-type BPN′ amino acid was judged to be optimal at any of the 12 positions. This was expected because stabilizing mutations at these sites had been found previously in the wild-type background. The gene for the initial parent subtilisin (Sbt88) had mutations at 2 of the 12 sites: Y217K and N218S. The screening re-identified serine as the optimal amino acid at 218. At position 217, L, V, Q, S, M, and Y were identified in the primary microtiter dish screen. Leucine at 217 was chosen for propagation based on its k_{cat}/K_m versus sAAPF-pNA, even though it is less stable than K217 and M217. Positions 166 and 222 also required a compromise between stability and catalytic activity. Serine was chosen at position 166 because of the 2.8-fold increase in half-life, even though catalytic turnover is 0.67 that of the wild-type G166. At position 222, glutamine was identified by random selection but reduced k_{cat}/K_m by 10-fold relative to the wild-type methionine. The M222Q mutant was selected for further study because removal of the peroxide-sensitive M222 from the active-site region of subtilisin makes the enzyme virtually insensitive to 1 M hydrogen peroxide (*30*, *35*, *36*). Table 2 summarizes the stability and kinetic data for all of the selected mutants. Mutations occurring at or near the substrate-binding surface have measurable effects on catalytic constants: I31L, E156S, G166S, G169A, A216E, K217L, and M222Q. The kinetic effects of these mutations are basically as anticipated from previous work (*7*). Mutations distal to the active site (S9A, S188P, N212G, and T254A) did not effect steady-state parameters. Contributions from the individual stabilizing mutations accrue cumulatively; thus, building a highly stable subtilisin was accomplished in a step by step manner by sequentially mutagenizing the Sbt88 gene and selecting the desired properties. All 12 mutations increase the half-life of calcium-free subtilisin at elevated temperature by 15 000-fold. Parallel mutagenesis and screening of 12 Sbt88 gene libraries would have been more expeditious had we not wished to examine the accumulated effects of stabilizing mutations on catalytic activity. Optimal mutations, once identified in the Sbt88 background, could have been combined to create stable, active mutants because of the independent effects of individual mutations. The strategy of

Table 2: Selection for Stability and Catalytic Activity[a]

parent strain	random site	observed mutations	k_{cat}/K_m (μM^{-1} s^{-1})	$t_{1/2}$ (65 °C)	$t_{1/2}$ (75 °C)
Sbt88	S218	S	0.35	400	0.3
		D	0.10	220	
		N*	0.17	83	
Sbt88	G169	A	1	2000	2
Sbt98 = (Sbt88 + A169)	E156	S	3		2.4
Sbt99 = (Sbt98 + S156)	K217	L	5.1		1.7
		V	2.5		0.5
		S	1.4		0.9
		Q	2.8		1.3
		M	2.7		2.6
		Y*	5.0		0.8
Sbt103 = (Sbt99 + L217)	T254	A	6		6
Sbt107 = (Sbt103 + A254)	I31	L	6		9.7
Sbt109 = (Sbt107 + L31)	G166	S	4		27
		R	5		18
Sbt110 = (Sbt109 + S166)	N212	G	4		41
Sbt116 = (Sbt110 + G212)	S188	P	4		53
Sbt140 = (Sbt116 + P188)	S9	A	4.2		95
Sbt151 = (Sbt140 + A9)	A216	E	4.7		160
Sbt153 = (Sbt151 + E216)	M222	Q (Sbt184)	0.45		450

[a] Steady-state kinetic parameters versus sAAPF-pNA were measured in 100 mM NaCl and 100 mM Tris-HCl at pH 8.3. Half-lives were measured in 100 mM NaCl and 100 mM Tris-HCl at pH 8.0, at an initial enzyme concentration of 1 μM. An asterisk denotes a reversion to the wild-type subtilisin BPN′ amino acid.

Table 3: Steady-State Kinetics[a]

subtilisin	K_m (μM)	k_{cat} (s^{-1})	k_{cat}/K_m (M^{-1} s^{-1})
	Substrate: sAAPF-pNA		
SBT*	450	210	0.47×10^6
Sbt140	48	190	4.0×10^6
Sbt151	45	190	4.2×10^6
Sbt153	46	218	4.7×10^6
Sbt184	300	134	0.45×10^6
	Substrate: G_BF30H		
subtilisin	K_m (μM)	k_{cat} (s^{-1})	k_{cat}/K_m (M^{-1} s^{-1})
SBT*	120	20	1.7×10^5
Sbt140	7	3.5	5.0×10^5
Sbt184	30	4.7	1.6×10^5
	Substrate: sAAF-AMC		
subtilisin	K_m (μM)	k_{cat} (s^{-1})	k_{cat}/K_m (M^{-1} s^{-1})
SBT*	360	6.4	0.16×10^5
Sbt140	63	26	4.1×10^5
	Substrate: sDVRAF-AMC		
subtilisin	K_m (μM)	k_{cat} (s^{-1})	k_{cat}/K_m (M^{-1} s^{-1})
SBT*	33	68	2.1×10^6
Sbt140	2.5	31	1.2×10^7
Sbt184	11.4	43	3.8×10^6

[a] Steady-state kinetic parameters were measured in 100 mM NaCl and 100 mM Tris-HCl at pH 8.3 and 25 °C. SBT* is a commercial version of sibtilisin BPN′ containing the Y217L mutation.

simultaneously mutagenizing all 12 sites in a single Sbt88 mutant library is not prudent because the size of the library ($\sim 4 \times 10^{15}$) is far too large to be screened effectively.

Analysis of Kinetic Properties versus sAAPF-pNA. The steady-state catalytic properties of the last four mutants in the series (Sbt140, Sbt151, Sbt153, and Sbt184) versus sAAPF-pNA are summarized in Table 3. Catalytic behavior is referenced against the Y217L variant of subtilisin BPN′. There are two reasons for this. First, it was found that interactions between the fluorogenic leaving group AMC and tyrosine 217 have large effects on the acylation rates observed for AMC substrates. Hence, for comparisons between substrates with pNA and AMC leaving groups, the Y217L mutant is a better reference enzyme. Second, the Y217L mutant is a commercial version of subtilisin BPN′ and is regarded as a better general protease (*37*). We found it to be more active than the wild-type enzyme against the range of substrates examined here. The Y217L mutant of subtilisin BPN′ will be denoted as SBT*. All stabilized variants, except Sbt184, were found to be more active than SBT* versus sAAPF-pNA (Table 3). However, none displayed more than 30% of the activity of SBT* against 1% casein. We investigated the reason for this behavior.

Scheme 1

$$E + S \underset{k_{-1}}{\overset{k_1}{\rightleftharpoons}} ES \xrightarrow{k_2} EP \underset{k_{-3}}{\overset{k_3}{\rightleftharpoons}} E + P$$

Analysis of Kinetic Properties versus the Protein Substrate. To obtain a more detailed assessment of catalytic properties versus a complex protein, we used a F30H mutant of the 56 amino acid IgG-binding domain of *Streptococcal* protein G as a substrate (*38*). The $\Delta G_{unfolding}$ of the mutant (denoted G_BF30H) is $\sim$2 kcal/mol at 25 °C; therefore, a single cut by a protease will cause the protein to unfold completely. Its unfolding can be followed by a 3-fold increase in fluorescence of its single tryptophan (*39*); thus, we were able to measure the kinetics of initial cleavage events. Table 3 shows steady-state kinetic parameters for SBT* and calcium-free mutants Sbt140 and Sbt184.

In terms of catalytic efficiency (k_{cat}/K_m), Sbt140 is better than SBT*. However, when the substrate concentration exceeds 15 μM (0.1 mg/mL), SBT* is better because its k_{cat} is almost 6 times higher than Sbt140. In fact, the peroxide-stable Sbt184 also has a higher k_{cat} than Sbt140. To understand this behavior, we employed transient-state kinetic methods to determine microscopic rate constants. A general kinetic scheme for subtilisin catalysis is as follows (Scheme

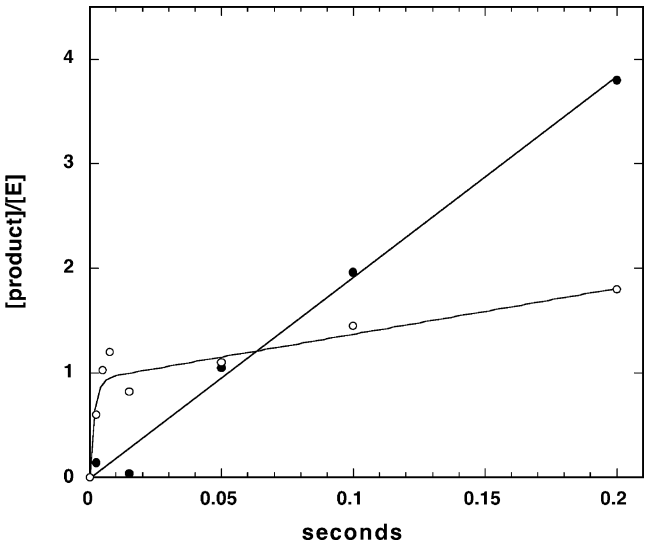

FIGURE 2: Pre-steady-state kinetics versus the G_BF30H substrate. Disappearance of the intact substrate as a ratio of [product]/[enzyme] is plotted versus time after mixing with SBT* (●) and Sbt140 (○).

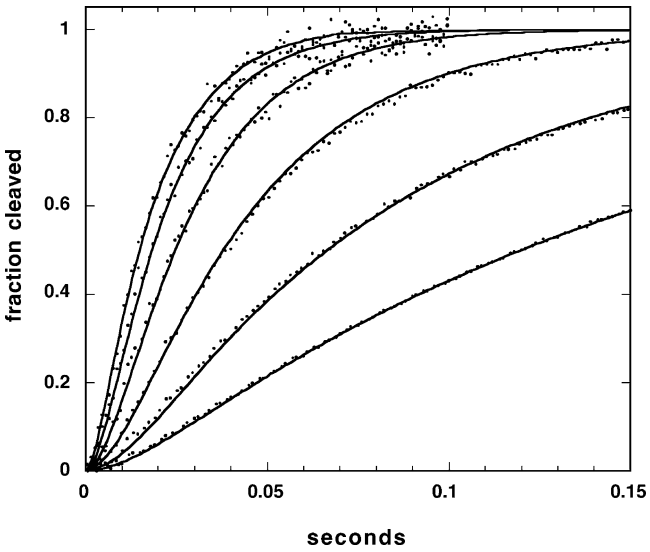

FIGURE 3: Single turnover kinetics of Sbt140 versus the sDVRAF-AMC substrate. Sbt140 subtilisin at [*E*] = 0.48, 1.05, 2.35, 5.05, 9.85, and 18.3 μM was mixed with 50 pM sDVRAF-AMC. The release of AMC is followed by fluorescence for each Sbt140 concentration. Solid lines are fits to Scheme 1 obtained with KinTekSim (*19*, *20*).

1)where *E* is the enzyme, *S* is the substrate, and *P* is the product. In this kinetic scheme, k_1 is the rate of substrate binding, k_{-1} is the rate of substrate dissociation, k_2 is the rate of the acylation, and k_3 is a composite rate constant including both deacylation and release of the N-terminal product. We were not able to detect an acyl intermediate in any of the subsequent quench-flow experiments with either G_BF30H or synthetic peptide substrates, and hence, we believe that the breakdown of the acyl intermediate is fast relative to the release of the peptide product. However, this has not been rigorously established.

Pre-Steady-State Kinetics. To find out why k_{cat} for SBT* is larger than k_{cat} for Sbt140, we measured pre-steady-state burst kinetics for both to determine the microscopic rate constants k_2 and k_3. In these experiments, subtilisin Sbt140 or SBT* is mixed with a saturating concentration (500 μM) of G_BF30H in a preparative quench-flow apparatus. The reaction is quenched after variable reaction times by mixing with H_3PO_4 to shift the pH to 2.0. Each reaction time point is run over an analytical FPLC column so that the disappearance of intact G_BF30H can be measured as a function of the reaction time.

With Sbt140, the time dependence for formation of cleaved product is described by a rapid exponential phase followed by a linear phase (Figure 2): [product]/[Sbt140] = $A_o(1 - e^{-\lambda t}) + k_{cat}t$, where rates are defined by $\lambda = k_2 + k_3 \sim 100\ s^{-1}$ and $k_{cat} = k_2k_3/(k_2 + k_3) = 4\ s^{-1}$. The amplitude of the burst phase (A_o) = $[k_2/(k_2 + k_3)]^2 = 0.9$. Solving these equations yields $k_2 \sim 100\ s^{-1}$ and $k_3 \sim 4\ s^{-1}$.

With SBT*, no pre-steady-state burst is observable. The time dependence for formation of the cleaved product is linear: [product]/[SBT*] = $k_{cat}t$, where $k_{cat} \sim k_2 = 20\ s^{-1}$.

These results indicate that the acylation in the reaction of Sbt140 with G_BF30H is rapid when compared to SBT* ($k_2 \sim 100\ s^{-1}$ versus $20\ s^{-1}$). The k_{cat} for Sbt140, however, is determined by k_3 ($\sim 4\ s^{-1}$).

Analysis of Kinetic Properties versus Succinyl-L-Asp-L-Val-L-Arg-L-Ala-L-Phe-7-amino-4-methylcoumarin (sDVRAF-AMC) and Succinyl-Ala-L-Ala-L-Phe-7-amino-4-methylcoumarin (sAAF-AMC). To further explore this phenomemon, we performed more detailed experiments using the defined, synthetic peptides: sDVRAF-AMC, which is a preferred subtilisin substrate, and sAAF-AMC, which is a poorer substrate. Steady-state parameters are summarized in Table 3. Sbt140 is a better enzyme versus sAAF-AMC than SBT* both in terms of k_{cat} and k_{cat}/K_m. The steady-state results with sDVRAF-AMC are qualitatively similar to the results with the G_BF30H substrate. That is, k_{cat}/K_m of Sbt140 is greater than SBT*, but the k_{cat} of Sbt140 is much lower. We also observed a burst phase in the reaction of Sbt140 with sDVRAF-AMC, indicating that acylation is not the rate-determining step. No burst phase was seen with sAAF-AMC.

Table 4: Microscopic Rate Constants versus sDVRAF-AMC[a]

	k_1 ($M^{-1}\ s^{-1}$)	k_{-1} (s^{-1})	k_2 (s^{-1})	k_3 (s^{-1})	K_S (μM)	K_m (μM)	k_{cat} (s^{-1})	K_P (μM)
Sbt140	1.6×10^7	15	65	60	0.94	2.5	31	8

[a] Transient-state kinetic parameters were measured in 100 mM NaCl and 100 mM Tris-HCl at pH 8.3 and 25 °C. Values for microscopic rate constants were determined by fitting the single turnover data in Figure 3.

We performed a series of single turnover experiments as a function of [*E*] to determine microscopic rate constants for a single pass through a catalytic cycle. [*E*] was varied from 0.5 to 18 μM with sDVRAF-AMC fixed at 50 pM. The data for Sbt140 were fit according to Scheme 1 using KinTekSIM (Figure 3). Steady-state, single turnover, and product inhibition data were used to determine the rate and equilibrium constants reported in Table 4.

The absence of a burst phase in the reaction of SBT* with sDVRAF at pH 8.3 indicates that acylation is limiting, as is generally observed for the hydrolysis of amide substrates by subtilisins. However, acylation is not the rate-determining step of the reaction of Sbt140 with sDVRAF-AMC. At pH 8.3, k_2 and k_3 are roughly equal, which causes k_{cat} to be half of the acylation rate.

Burst-phase kinetics with amide substrates generally have not been reported with subtilisins because of a focus on

steady-state analysis and because the acylation step is rate-limiting for the commonly used peptide substrates such as sAAPF-pNA. No burst phase is observed when Sbt140 is reacted with sAAPF-pNA. We estimate that the k_3 for sAAPF is $\sim 10^3$ s^{-1}. Because k_3 greatly exceeds the rate of acylation, it does not influence the overall kinetics. Burst kinetics have been observed for the yeast-processing subtilisin, Kex2, against cognate sequences (*40*, *41*).

DISCUSSION

Substrate Binding and N-Terminal Product Release. Degradative subtilisins have evolved to be efficient catalysts against a broad range of substrate sequences. Subtilisin can bind to a broad range of sequences because many of its interactions are with the peptide backbone of the substrate. Most contacts are with the first four substrate residues on the acyl side of the scissile bond. These are denoted P1−P4, with numbering from the scissile bond toward the N terminus of the substrate (*42*−*44*). The backbone of the substrate inserts between strands 100−104 and 125−129 of subtilisin to become the central strand in an antiparallel β-sheet arrangement involving seven main-chain hydrogen bonds (*8*, *43*). Hence, a major component of substrate-binding energy involves only the peptide backbone and not side-chain interactions. The side-chain components of substrate binding to subtilisin result primarily from the P1 and P4 amino acids (*5*, *24*, *45*). Optimal substrates for subtilisin have large hydrophobic amino acids at these positions (*24*, *45*), but even a substrate with AAAA at P1−P4 would be expected to bind with a K_S of <10 μM (*24*, *26*, *46*, *47*).

It is frequently viewed as axiomatic that $k_{cat} \sim k_2$ for subtilisins (*24*). For the stabilized subtilisin Sbt140, this was true for the substrates, sAAF-AMC and sAAPF−PNA, but was not true for the preferred substrate sDVRAF-AMC or for the complex protein substrate G_BF30H. In both of these cases, tight substrate binding appears be correlated with slow product release. The effects of slow product release on steady-state kinetics can be discerned by examining the steady-state rate according to Scheme 1. If the rate of product release is much faster than acylation then

$$k_{cat} \sim k_2$$

and

$$K_m \sim (k_2 + k_{-1})/k_1$$

However, if k_3 is in the same range as k_2, then both k_{cat} and K_m will be decreased by a factor of $k_3/(k_2 + k_3)$. Slow product release is not manifest in the ratio of k_{cat}/K_m, which frequently is used as a measure of catalytic efficiency. By this measure, Sbt140 subtilisin is a more efficient enzyme than SBT* across a range of substrates: sAAPF-pNA, sAAF-AMC, sDVRAF-AMC, and G_BF30H. However, the value of k_{cat} for Sbt140 subtilisin for a "good" peptide substrate such as sDVRAF-AMC or a complex protein such as G_BF30H is much worse than SBT*. The reasons for this behavior can be seen by examining the microscopic rate constants for the hydrolysis of sDVRAF-AMC.

The ratio k_{cat}/K_m is the apparent second-order rate constant for substrate binding. It is less than the true binding rate (k_1) by a factor of $k_2/(k_2 + k_{-1})$ (*48*). For the reaction of Sbt140 with sDVRAF-AMC, $k_{cat}/K_m \sim k_1$ because the substrate off rate is small ($k_{-1} = 15$ s^{-1}), compared to the acylation rate ($k_2 = 65$ s^{-1}). As the substrate off rate becomes less than the acylation rate, its influence on the observed rate of product formation diminishes because of tight kinetic coupling between substrate binding and acylation. Further, because the slow substrate off rate is correlated to the slow release of the N-terminal product, k_{cat} is attenuated. Thus, substrate affinity above a certain threshold is detrimental to catalysis, even though it has no effect on k_{cat}/K_m.

Tight-binding peptides, such as sDVRAF-AMC, appear to be better indicators of activity against a complex protein substrate than an average peptide such as sAAPF-pNA. The reaction of Sbt140 with G_BF30H is characterized by a rapid burst phase followed by a much slower steady-state phase. As with sDVRAF-AMC, Sbt140 appears to bind tightly to preferred sequences in G_BF30H and to release N-terminal products slowly. Interestingly, this effect can be mitigated by the mutation M222Q. This mutation decreases the acylation rate by a factor of 1.6 but increases k_{cat} because of a concomitant increase in k_3. This mutation is of interest because it makes the enzyme stable in hydrogen peroxide because of the removal of the oxidation-sensitive methionine. (*30*).

Stability and Catalytic Activity. The insertion of the substrate between subtilisin strands 100−104 and 125−129 to become the central strand in an antiparallel β-sheet arrangement suggests that increased subtilisin stability might result in tighter substrate binding. However, this does not appear to be the case. The kinetic behavior observed with Sbt140 subtilisin does not appear to be a function of stability but rather to be dependent on specific mutations, which directly alter substrate and product interactions. The mutation that has the largest effect on substrate binding is E156S. This mutation has a minor effect on stability but amplifies the natural preference of subtilisin for large hydrophobic residues at the P1 site by 2−5-fold (*26*). The additive effects of E156S, G169A, and N218S increase substrate affinity by ~15-fold and together create an enzyme whose k_{cat} is attenuated by product release in the presence of high-affinity substrates. The effect is mitigated to some extent by Y217L, which increases the acylation rate by ~5-fold and decreases K_S by ~5-fold. Y217L effects on k_{cat} and K_m depend on k_{-1} and k_3 for a particular substrate. The kinetic properties of Sbt140 appear to be roughly similar to the S156, A169, and L217 mutants of BPN′ described by Wells et al. (*26*). Natural evolution appears to compromise between substrate binding versus acylation rate. In most *Bacillus* subtilisins, Y217 and E156 occur together or L218 and S156 occur together (*49*). Natural subtilisins may require a great deal of versatility to deal with folded and unfolded substrates over a range of concentrations. Preservation of broad proteolytic activity requires that N-terminal off rates do not attenuate k_{cat}. It is possible, however, to tailor the catalytic profile to create a more specialized protease. For example, Sbt140 is a very good protease in situations in which tight substrate affinity is important (e.g., substrates at low concentration, of non-optimal sequence, or in folded conformation). Tailoring of the catalytic profile appears to be compatible with high protease stability. We recently have been able to extend this work to evolve subtilisins with narrow substrate preferences to create useful processing activities in subtilisin (*50*).

ACKNOWLEDGMENT

The authors thank Feng Hong Song for synthesizing the oligonucleotides used in site-directed mutagenesis and DNA sequencing.

REFERENCES

1. Ottesen, M., and Svendsen, I. (1970) The subtilisins, *Methods Enzymol. 19*, 199−215.
2. Wells, J. A., Ferrari, E., Henner, D. J., Estell, D. A., and Chen, E. Y. (1983) Cloning, sequencing, and secretion of *Bacillus amyloliquifaciens* subtilisin in *Bacillus subtilis*, *Nucleic Acids Res. 11*, 7911−7925.
3. Vasantha, N., Thompson, L. D., Rhodes, C., Banner, C., Nagle, J., and Filpula, D. (1984) Genes for alkaline and neutral protease from *Bacillus amyloliquifaciens* contain a large open-reading frame between the regions coding for signal sequence and mature protein, *J. Bacteriol. 159*, 811−819.
4. Bryan, P. N. (2000) Protein engineering of subtilisin, *Biochim. Biophys. Acta 1543*, 203−222.
5. Gron, H., Meldal, M., and Breddam, K. (1992) Extensive comparison of the substrate preferences of two subtilisins as determined with peptide substrates which are based on the principle of intramolecular quenching *Biochemistry 31*, 6011−6018.
6. Sroga, G. E., and Dordick, J. S. (2001) Generation of a broad esterolytic subtilisin using combined molecular evolution and periplasmic expression, *Protein Eng. 14*, 929−937.
7. Zhao, H., and Arnold, F. H. (1999) Directed evolution converts subtilisin E into a functional equivalent of thermitase, *Protein Eng. 12*, 47−53.
8. McPhalen, C. A., and James, M. N. G. (1988) Structural comparison of two serine proteinase-protein inhibitor complexes: Eglin-C-subtilisin Carlsberg and CI-2-subtilisin novo, *Biochemistry 27*, 6582−6598.
9. Bryan, P., Alexander, P., Strausberg, S., Schwarz, F., Wang, L., Gilliland, G., and Gallagher, D. T. (1992) Energetics of folding subtilisin BPN′, *Biochemistry 31*, 4937−4945.
10. Gallagher, T. D., Bryan, P., and Gilliland, G. (1993) Calcium-free subtilisin by design, *Proteins: Struct., Funct., Genet. 16*, 205−213.
11. Almog, O., Gallagher, T., Tordova, M., Hoskins, J., Bryan, P., and Gilliland, G. L. (1998) Crystal structure of calcium-independent subtilisin BPN′ with restored thermal stability folded without the prodomain, *Proteins 31*, 21−32.
12. Strausberg, S., Alexander, P., Gallagher, D. T., Gilliland, G., Barnett, B. L., and Bryan, P. (1995) Directed evolution of a subtilisin with calcium-independent stability, *BioTechnology 13*, 669−673.
13. Almog, O., Gallagher, D. T., Ladner, J. E., Strausberg, S., Alexander, P., Bryan, P., and Gilliland, G. L. (2002) Structural basis of thermostability. Analysis of stabilizing mutations in subtilisin BPN′, *J. Biol. Chem. 277*, 27553−27558.
14. Fahnestock, S. R., and Fisher, K. E. (1987) Protease-deficient *Bacillus subtilis* host strains for production of *Staphylococcal* protein A, *Appl. Environ. Microbiol. 53*, 379−384.
15. Alexander, P. A., Ruan, B., Strausberg, S. L., and Bryan, P. N. (2001) Stabilizing mutations and calcium-dependent stability of subtilisin, *Biochemistry 40*, 10640−10644.
16. Pantoliano, M. W., Whitlow, M., Wood, J. F., Dodd, S. W., Hardman, K. D., Rollence, M. L., and Bryan, P. N. (1989) Large increases in general stability for subtilisin BPN′ through incremental changes in the free energy of unfolding, *Biochemistry 28*, 7205−7213.
17. Alexander, P. A., Ruan, B., and Bryan, P. N. (2001) Cation-dependent stability of subtilisin, *Biochemistry 40*, 10634−10639.
18. DelMar, E., Largman, C., Brodrick, J., and Geokas, M. (1979) A sensitive new substrate for chymotrypsin, *Anal. Biochem. 99*, 316−320.
19. Zimmerle, C. T., and Frieden, C. (1989) Analysis of progress curves by simulations generated by numerical integration, *Biochem. J. 258*, 381−387.
20. Barshop, B. A., Wrenn, R. F., and Frieden, C. (1983) Analysis of numerical methods for computer simulation of kinetic processes: Development of KINSIM−A flexible, portable system, *Anal. Biochem. 130*, 134−145.
21. Takagi, H., Morinaga, Y., Ikemura, H., and Inouye, M. (1988) Mutant subtilisin E with enhanced protease activity obtained by site-directed mutagenesis, *J. Biol. Chem. 263*, 19592−19596.
22. Sternberg, M. J., Hayes, F. R., Russell, A. J., Thomas, P. G., and Fersht, A. R. (1987) Prediction of electrostatic effects of engineering of protein charges, *Nature 330*, 86−88.
23. Wells, J. A., Powers, D. B., Bott, R. R., Graycar, T. P., and Estell, D. A. (1987) Designing substrate specificity by protein engineering of electrostatic interactions, *Proc. Natl. Acad. Sci. U.S.A. 84*, 1219−1223.
24. Estell, D. A., Graycar, T. P., Miller, J. V., Powers, D. B., Burnier, J. P., Ng, P. G., and Wells, J. A. (1986) Probing steric and hydrophobic effects on enzyme−substrate interactions by protein engineering, *Science 233*, 659−663.
25. Rollence, M. L., Filpula, D., Pantoliano, M. W., and Bryan, P. N. (1988) Engineering thermostability in subtilisin BPN′ by *in vitro* mutagenesis, *CRC Crit. Rev. Biotechnol. 8*, 217−224.
26. Wells, J. A., Cunningham, B. C., Graycar, T. P., and Estell, D. A. (1987) Recruitment of substrate-specificity properties from one enzyme into a related one by protein engineering, *Proc. Natl. Acad. Sci. U.S.A. 84*, 5167−5171.
27. Miyazaki, K., and Arnold, F. H. (1999) Exploring nonnatural evolutionary pathways by saturation mutagenesis: Rapid improvement of protein function, *J. Mol. Evol. 49*, 716−720.
28. Brode, P. F., III, Erwin, C. R., Rauch, D. S., Barnett, B. L., Armpriester, J. M., Wang, E. S., and Rubingh, D. N. (1996) Subtilisin BPN′ variants: Increased hydrolytic activity on surface-bound substrates via decreased surface activity, *Biochemistry 35*, 3162−3169.
29. Bryan, P. N., Rollence, M. L., Pantoliano, M. W., Wood, J., Finzel, B. C., Gilliland, G. L., Howard, A. J., and Poulos, T. L. (1986) Proteases of enhanced stability: Characterization of a thermostable variant of subtilisin, *Proteins: Struct., Funct., Genet. 1*, 326−334.
30. Estell, D. A., Graycar, T. P., and Wells, J. A. (1985) Engineering an enzyme by site-directed mutagenesis to be resistant to chemical oxidation, *J. Biol. Chem. 260*, 6518−6521.
31. Heringa, J., Argos, P., Egmond, M. R., and de Vlieg, J. (1995) Increasing thermal stability of subtilisin from mutations suggested by strongly interacting side-chain clusters, *Protein Eng. 8*, 21−30.
32. Narhi, L. O., Stabinsky, Y., Levitt, M., Miller, L., Sachdev, R., Finley, S., Park, S., Kolvenbach, C., Arakawa, T., and Zukowski, M. (1991) Enhanced stability of subtilisin by three point mutations, *Biotechnol. Appl. Biochem. 13*, 12−24.
33. Cunningham, B. C., and Wells, J. A. (1987) Improvement in the alkaline stability of subtilisin using an efficient random mutagenesis and screening procedure, *Protein Eng. 1*, 319−325.
34. Sears, P., Schuster, M., Wang, P., Witte, K., and Wong, C.-H. (1994) Engineering subtilisin for peptide coupling: Studies on the effects of counterions and site-specific modifications on the stability and specificity of the enzyme, *J. Am. Chem. Soc. 116*, 6521−6530.
35. Stauffer, C. E., and Etson, D. (1969) The effect on subtilisin activity of oxidizing a methionine residue, *J. Biol. Chem. 244*, 5333−5338.
36. Bott, R., Ultsch, M., Kossiakoff, A., Graycar, T., Katz, B., and Power, S. (1988) The three-dimensional structure of *Bacillus amyloliquefaciens* subtilisin at 1.8 Å and an analysis of the structural consequences of peroxide inactivation, *J. Biol. Chem. 263*, 7895−7906.
37. Wolff, A. M., Showell, M. S., Venegas, M. G., Barnett, B. L., and Wertz, W. C. (1996) Laundry performance of subtilisin proteases, *Adv. Exp. Med. Biol. 379*, 113−120.
38. Sari, N., Alexander, P., Bryan, P. N., and Orban, J. (2000) Structure and dynamics of an acid-denatured protein G mutant, *Biochemistry 39*, 965−977.
39. Alexander, P., Orban, J., and Bryan, P. (1992) Kinetic analysis of folding and unfolding the 56 amino acid IgG-binding domain of *Streptococcal* protein G, *Biochemistry 31*, 7243−7248.
40. Rockwell, N. C., and Fuller, R. S. (2001) Differential utilization of enzyme−substrate interactions for acylation but not deacylation during the catalytic cycle of Kex2 protease, *J. Biol. Chem. 276*, 38394−38399.
41. Rockwell, N. C., and Fuller, R. S. (2001) Direct measurement of acylenzyme hydrolysis demonstrates rate-limiting deacylation in cleavage of physiological sequences by the processing protease Kex2, *Biochemistry 40*, 3657−3665.

42. Berger, A., and Schechter, I. (1970) Mapping the active site of papain with the aid of peptide substrates and inhibitors, *Philos. Trans. R. Soc. London, Ser. B 257*, 249−264.
43. McPhalen, C. A., Schnebli, H. P., and James, M. N. (1985) Crystal and molecular structure of the inhibitor eglin from leeches in complex with subtilisin Carlsberg, *FEBS Lett. 188*, 55−58.
44. Bode, W., Papamokos, E., Musil, D., Seemueller, U., and Fritz, H. (1986) Refined 1.2 Å crystal structure of the complex formed between subtilisin Carlsberg and the inhibitor eglin c. Molecular structure of eglin and its detailed interaction with subtilisin, *EMBO J. 5*, 813−818.
45. Gron, H., and Breddam, K. (1992) Interdependency of the binding subsites in subtilisin, *Biochemistry 31*, 8967−8971.
46. Ballinger, M. D., Tom, J., and Wells, J. A. (1995) Designing subtilisin BPN′ to cleave substrates containing dibasic residues, *Biochemistry 34*, 13312−13319.
47. Rheinnecker, M., Baker, G., Eder, J., and Fersht, A. R. (1993) Engineering a novel specificity in subtilisin BPN′, *Biochemistry 32*, 1199−1203.
48. Johnson, K. A. (1992) Transient-state kinetic analysis of enzyme reaction pathways, *Enzymes 20*, 1−61.
49. Siezen, R. J., and Leunissen, J. A. (1997) Subtilases: The superfamily of subtilisin-like serine proteases, *Protein Sci. 6*, 501−523.
50. Ruan, B., Fisher, K. E., Alexander, P. A., Doroshko, V., and Bryan, P. N. (2004) Engineering subtilisin into a fluoride-triggered processing protease useful for one-step protein purification, *Biochemistry 43*, 14539−14546.

BI047806M